

Computer Vision System for Weld Bead Analysis

Luciane Baldassari Soares, Atila Astor Weis, Bruna de Vargas Guterres, Ricardo Nagel Rodrigues
and Silvia Silva da Costa Botelho

Science Computer Center - C3, Federal University of Rio Grande - FURG, Brazil

Keywords: Computer Vision, Discontinuities, Welding.

Abstract: Welding processes are very important in different industries and requires precision and attention in the steps that will be performed. This article proposes the use of an autonomous weld bead geometric analysis system in order to verify the presence of geometric failures that may compromise the weld integrity. Using an vision system attached to a linear welding robot, images of pre-welded and post-welded metal plates are captured and compared and metrics are applied for evaluation. The proposed method uses Hidden Markov Model (HMM) to identify the weld bead edges and calculate several evaluation metrics to detect geometric failures such as misalignment, lack or excess of fusion, among others.

1 INTRODUCTION

The Welding process consists of a fundamental practice in several areas such as automotive industry, metallurgy, civil construction, naval industry and railway. The welding process is considered laborious due to the risks the welder is exposed to, such as sparks, toxic gases, radiation emitted by the arc and electricity. For this reason, technological advances in this area not only provide productivity increase and process enhancement, but also assure the welder security. Besides the mentioned risks, the welder must adjust the parameters, guide the torch and control the weld bead quality (Broering et al., 2005). As a consequence, the weld quality and the productivity may be compromised since the operator can become over-worked.

Welding processes represent a very significant part of the manufacturing costs of a product. Therefore a weld bead fault not identified during the quality inspection process can have major consequences for the equipment manufacturer (Andreucci, 2013).

Due to all above mentioned factors, the use of human operated welding robots is increasingly common. Additionally, these robots reduce the rework and provide a more efficient production line. In the naval industry, for example, it is indispensable to use more flexible solutions since it is necessary to weld metal sheets for different sized ships.

In shipyards, an alternative to automate the welding process is the Bug-O Matic Weaver robot, shown

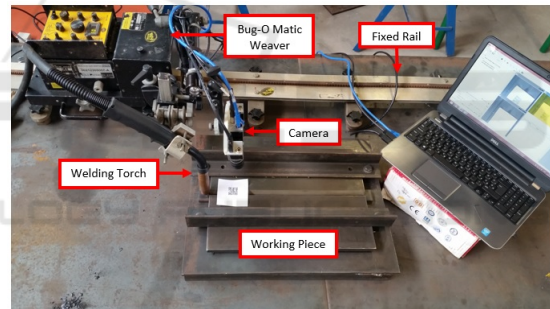


Figure 1: Bug-O Matic Weaver Robot - Source: Author.

in Figure 1. The system is remotely operated, decreasing the welder contact with the risk area. The robot, positioned on a rail attached to any linear surface, carries the torch during the welding process. It is possible to set different parameters such as weaving regime (arm oscillatory movement) and robot and arm linear velocity.

It is worth noting the predominant welding technique used in shipyards is the *FCAW (Flux Cored Arc Welding)*. The FCAW has several advantages being widely used in naval industry which aims to increase the productivity keeping the quality of the processes (Machado, 2015).

The automation of the welding process makes it not only more stable, but also more uniform, thus reducing the risks of discontinuities and avoiding the weld bead discard (Carvalho et al., 2009). Furthermore, to manually achieve this quality level it would

be necessary a welder with years of experience.

Nowadays, the weld bead inspection is performed not only by Non-Destructive Testing (NDT) including visual methods, penetrating liquid, magnetic particles, radiography and ultrasound, but also by Destructive Evaluation such as tensile, impact, folding, fatigue and hardness tests (Lima et al., 2005). According to (Andreucci, 2013), the solution to assist the quality control of equipments and materials is related to NDT techniques. As reported by the Brazilian Association of Non-Destructive Testing and Inspection (ABENDI), the NDT techniques are one of the main quality control tools, they increase the weld reliability and reduce the process cost (Abendi, 2014).

It is important for the realized tests the identification of discontinuities such as incomplete or excessive fusion, welding bite, porosity, incomplete or excessive penetration, cracks and geometrical weld bead irregularities that may compromise the weld quality. Although it is possible to extract some relevant information about the weld bead geometry, we still do not have a tool able to identify all presented discontinuities.

The computer vision may be the solution to quickly and precisely identify some of the above discontinuities. In conclusion, computational techniques are studied and applied in order to establish an automatic and ideal solution for the inspection and detection of discontinuities on the weld seam (Felisberto, 2010).

2 LITERATURE REVIEW

In the works (Cook et al., 1995; Hou and Liu, 2012; Kumar et al., 2012; Kumar et al., 2014) it is presented methods offline for welding quality inspection and evaluation using digital cameras and lighting system. More classic approaches are carried out in (Cook et al., 1995) and (Hou and Liu, 2012). It is assumed that the weld width (which can be identified through the horizontal integration) and the spacing between the undulations (which can be obtained through the peak-to-peak distance) can not oscillate for good weld quality. Moreover Hou *et al.* makes use of the Canny algorithm for identifying the edges of the weld bead. After the edges are identified, they are plotted in 2D histogram, in order to compare them with histograms of images of good quality weld beads. Through a pre-established threshold the weld is classified good or not.

In the article of Kumar *et al.* (Kumar et al., 2012)(Kumar et al., 2014) an evaluation system for MIG (Metal Inert Gas) welding in “V” groove is pro-

posed. Four frames are captured in sequence and then the regions of interest of the image are segmented and some characteristics based on the average intensity of the pixels are extracted. In (Kumar et al., 2012), the authors use a back-propagation neural network to classify the weld in four categories: good, excessive, insufficient and without weld. The system was tested with 80 samples and shows 95% accuracy in the classification. Yet, in (Kumar et al., 2014) the same classifier was used but with improved feature extraction, based on a chi-square test to verify compliance with a Gaussian distribution of pixels. This increased precision to 96.25%.

In the articles on (Schreiber et al., 2009) and (Sun et al., 2005) the visual inspection methods are applied online, that is, they are performed during the welding process. In these methods the camera is usually placed next to the torch, obtaining an image of the recently welded bead. The biggest obstacle to online processing is the acquisition of images due to conditions in the welding environment such as arc brightness, smoke, sparks, welding spatters and reflections.

The works of Schreiber *et al.* and Sun *et al.* use training techniques and pattern recognition, so that the algorithm learns the good and bad characteristics of a weld bead. Schreiber *et al.* presents a system that consists of two distinct phases: training and verification. In the training phase the system learns the quality criterion required from the training performed through images of weld beads considered to be well welded, examined by a welding engineer. This step should be performed only once before using the robot and consists of extracting measurements from the images of the training weld beads. These measures are combined in order to obtain reference values and tolerance ranges.

The verification step occurs by comparing each frame obtained from the image of the welding being performed, with the reference frames obtained from the weld beads of training. In this process the evaluated characteristics are the position and the width of the cord, as well as the distribution of light around the arc.

Sun *et al.* proposes a method of visual inspection using a Fuzzy Pattern Recognition algorithm. The method can detect defects such as porosity, lack of penetration and lack of material in the weld bead. If the defect exceeds the established minimum standard, the system will automatically send an alarm and mark the position where defects appear to help workers repair them. The system is efficient since the speed of detection can reach 3-4 frames per second. It was reported that the method identified 65 of the 66 defects included in the test set.

As described in the works above, the acquisition and processing of images of the online weld bead becomes much more difficult due to environmental conditions. Because of this, we often end up missing important information from the weld bead image, so in this research we opted for offline analysis. Between the techniques studied for weld bead discontinuity analysis, the (Schreiber et al., 2009) method and (Sun et al., 2005) method had a great contribution to our research since we followed the same training and verification behavior as we can see in the next section.

3 METHODOLOGY

The edge analysis is based on the the empty groove characteristics. Through the proposed method it is possible to detect the discontinuities shown on Figure 2 wich are misalignments along the weld bead, angular misalignments, excessive and insufficient material deposition.

Firstly, images were taken from several weld seam which qualities vary between acceptable or not. They were taken using a camera with an passive illumination system (green leds) which is perpendicularly attached to the proof body. The distance between them is 15 cm providing a top view of the interest area.

In conclusion, a computer visual system is proposed in order not only to highlight the weld bead edges, but also to analyze its geometry and detect some discontinuities. Furthermore, through a combination of existent techniques such as PCA (*Principal Component Analysis*) to assist the data reduction, Gaussian mixture as a probabilistic method and HMM (*Hidden Markov Model*) as a statistical model, a edge detection system is composed. The method execution is illustrated on Figure 3. In addition, the MATLAB (Matrix Laboratory) software was used to develop the system due to its facility for parameters testing.

The method can be divided on two stages: training and testing. In the training stage several weld bead images are presented in order to make the system learn to identify not only good quality edges, but also discontinuities. The testing stage consists on the pos-weld verification on wich the weld bead edges are highlighted and the metrics, present in the section 4, are applied. Through this stage it is possible to assist not only the welder, but also the inspector to identify discontinuities that may cause the weld bead invalidation.

3.1 Training

This stage encompasses the image capture of different weld processes performed by the Bug-O Matic Weaver robot with not only acceptable quality but also discontinuities. The obtained images are used as ground-thruth and its edges are manually marked.

At a first moment, the edges of three weld bead images of 3288 pixels height by 4608 pixels wide were highlighted. Thus we have a total of 19728 annotated lines since each image has a 3288 pixels height and two annotated edges. Therefore, each image provides 6576 samples and 19728 edge points samples, called edges profile, since each annotated point is located on a single line.

For each point along the edge an edge profile is extracted consisting on β pixels on the right and β pixels on the left of the annotated edge. The edge profile represents each pixel intensity and its concept is exemplified on Figure 4. After extraction of all edge profiles, there is a set of vectors that will be used to learn the edge model. Thus, $\beta = 80$ is used.

Applying the PCA technique in the set of edge profiles possible overlaps are reduced thus obtaining a reduction in the data without significant loss of information. It is used 85 % of the total variance of the analyzed components resulting on a PCA size of nineteen.

The PCA space edge profiles projections are used to train a gaussian mixture. The equation 1 represents the probability of a given projection being an edge.

$$P(x|\theta) = \sum_{i=1}^k w_i g(x|\mu_i, \Sigma_i), \quad (1)$$

Where $w_i = 1, 2, \dots, k$ are the k components wheights, μ_i represents an D-dimensional mean vector and Σ_i is a covariance matrix.

The Gaussian mixture parameters are learned by a Maximum Likelihood Algorithm (*Expectation Maximization - EM*) which is a parameter estimation technique that allow to deal with missing data. Furthermore, the number of Gaussians k was set to seven since the *BIC* (*Bayesian Information Criterion*) presents a graphical stable behavior at this value when a 1-30 range is analyzed.

It is emphasized that these images are used only in the training, the test stage makes use of new images of other weld processes performed by the same robot.

3.2 Tests

After training the proposed method, the testing stage is performed. To evaluate the proposed method, the detection of the weld beads edges are oerformed in

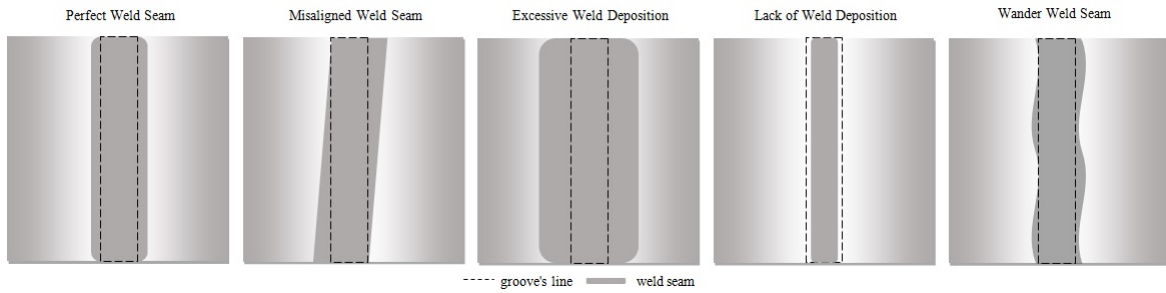


Figure 2: Weld beads geometry.

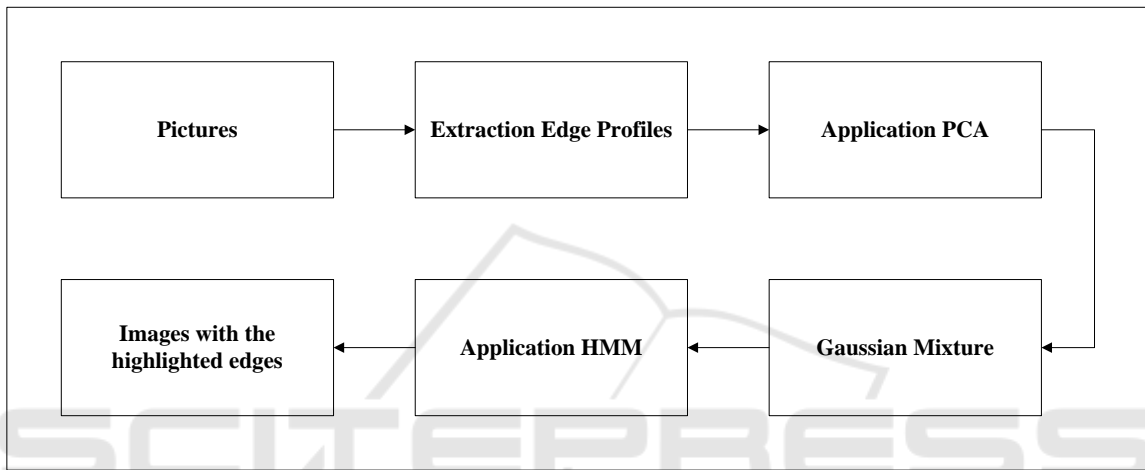


Figure 3: The proposed method block diagram.

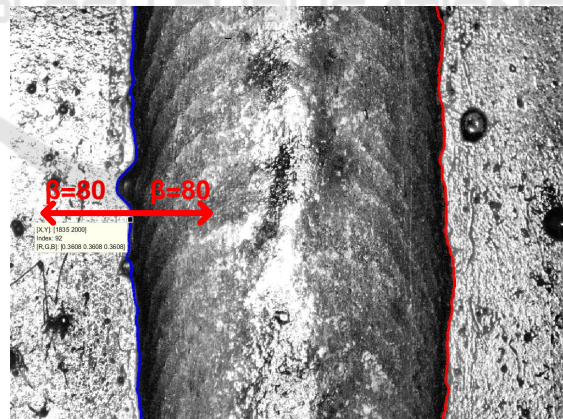
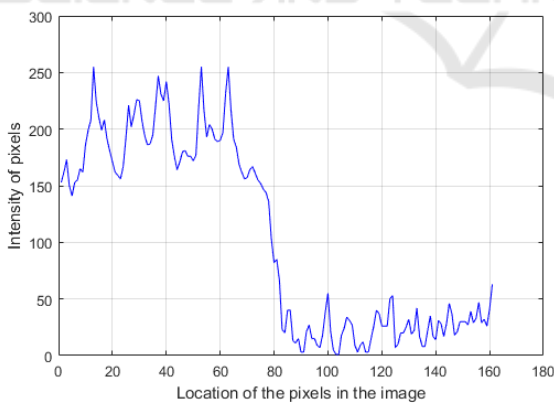


Figure 4: Right edge image profile graphically represented.

different images that were not used to train the proposed method. For this purpose, the *HMM* technique is used since it is a statistical model on which the modeling system is a Markov process with unknown parameters. Furthermore, it provides the hidden parameters knowledge based on the observable ones. The model extracted parameters can be used to realize new analysis such as pattern recognition (Anzai,

2012) which is the main purpose of its implementation.

For each given image, a region of interest (*ROI*) is determined considering 250 pixels for each side of the empty groove position. It assists to calculate the probability of a pixel being an edge or not.

Furthermore, the edge position along the image lines follows a Markov model. It means that given the

edge position at line $t - 1$ the probability of its position at line t , $p(y_t|y_{t-1})$ is obtained. The transition models are defined by the equations:

$$p(y_t = y_{t-1}) = 0,9 \quad (2)$$

$$p(y_t = y_{t-1} - 1) = 0,05 \quad (3)$$

$$p(y_t = y_{t-1} + 1) = 0,05 \quad (4)$$

In conclusion, the appearance model $p(x|y)$ consists in estimating the probability of the variable y being an edge x . Thus, based on the observable data (edge profile of the weld bead images defined as x) the hidden variables (edge position along the weld bead) are estimated. It means the *HMM* is responsible for inferring the edge profile location on the new weld bead image.

By means of Viterbi algorithm, edge position sequence estimation is realized. Moreover, it is necessary to identify the next states on a excellent way justifying the implementation of the Viterbi algorithm since it is a optimal search algorithm as can be seen on Equation 5.

$$y^* = \arg_y \max p(y|x) \quad (5)$$

After this stage, tests are performed on new images from the testing set. The region of interest is selected based on the empty groove position. It allows to analyze smaller areas of the image enhancing the time aspect of its processing. Finally, the probability of each pixel within the ROI being an edge is analyzed.

4 EVALUATION METRICS

The proposed metrics aim to identify some discontinuities shown on Figure 2 such as lack or excess of weld deposition and misalignments along the weld bead. The applied metrics are: minimum, maximum and average distance between the edges and the empty groove position, weld bead standard deviation along the edge using the sliding window method and angle between the edge and the empty groove using the same method. It is worth mentioning the sliding window method consists on analyzing adjustable sized portions of the ROI (window) along its height.

Through the method developed by (Steffens et al., 2016) the empty groove lines are captured for later comparison with the filled one. The mentioned author uses the LSD (Line Segment Detector) algorithm to correctly find the empty groove lines since it shows

major performance to other methods in detecting lines in metal sheets. Furthermore, the proposed algorithm realizes the lines filtering only keeping the vertical ones. The weld parameters, which encompasses electric current and voltage, wire feed rate, robot linear velocity and oscillation type and velocity, are automatically determined after extracting the empty groove lines. Hereafter, the *FCAW* welding process is initiated by the Bug-O Matic Weaver robot requiring four steps for the groove complete filling.

After the welding process is finished, the weld bead is imaged and, finally, the proposed method provides the weld bead edges detection. Soon after, geometric evaluation visual metrics are implemented for discontinuities verification.

4.1 Minimum Value

The first implemented metric, as can be seen on Equation 6, consists on the minimum distance between the weld bead edge and the empty groove line for both sides of the weld bead. Through this metric it is possible to identify regions with lack of material deposition.

$$M_1 = \min |Y_i - C_i| \quad (6)$$

Where $i = 1...n$ represents the analyzed image line, Y_i refers to the edge position on the image and C_i is the groove position.

4.2 Maximum Value

The considered metric consists on the maximum distance between the weld bead edge and the empty groove line for both sides of the weld bead as shown in Equation 7. This metric allows the identification of regions with excessive material deposition.

$$M_2 = \max |Y_i - C_i| \quad (7)$$

Where $i = 1...n$ represents the analyzed image line, Y_i refers to the edge position on the image and C_i is the groove position.

4.3 Average Value

This metric consists on the average distance between the weld bead edge and the empty groove line for both sides of the weld bead as shown in Equation 8. This metric assists the analysis of the weld bead regularity since a pattern without considerable oscillations is desired.

$$M_3 = \frac{\sum_{i=1}^n |Y_i - C_i|}{n} \quad (8)$$

Where $i = 1 \dots n$ represents the analyzed image line, Y_i refers to the edge position on the image and C_i is the groove position.

4.4 Standard Deviation using sliding window

This metric consists on calculating the standard deviation using the sliding window method with size w as shown in equation 9. Its application assists the identification of misalignments points along the weld bead edge.

$$M_4(k) = \sqrt{\frac{\sum_{i=k}^{k+w-1} (Y_i - C_i - \frac{\sum_{j=k}^{k+w-1} |Y_j - C_j|}{t})^2}{w}} \quad (9)$$

Where n represents the image lines quantity, w is the window size, $k = \{1 \dots n - w\}$, Y_i refers to the edge position on the image and C_i is the groove position.

4.5 Angle between Empty Groove and Weld Bead Edge using sliding window

Aiming to obtain the angle between the empty groove and the edge for both sides the weld bead, it is used a linear regression method. This way, both the linear and angular coefficients of the groove and the edge approximate lines are obtained. Thus, the Equation 10 allows to calculate the desired angle. Through this metric it is possible to identify if the weld bead exhibits angular misalignments with respect to the empty groove.

$$M_5 = \arctan \left| \frac{a_c - a_y}{1 + a_c \cdot a_y} \right| \quad (10)$$

Where a_c is the angular coefficient of the empty groove approximated line and a_y is the angular coefficient of the weld bead approximated line both with respect to the analyzed window.

5 RESULTS

This section is divided in two parts. Firstly, the weld bead edge identification method results are presented. Secondly, the results of the evaluation metrics application, as described on section 4, are discussed.

5.1 Proposed Method

In this section some images with highlighted edges are presented. It is worth mentioning the highlighted edges were identified by the proposed method. Thus, at the left side of Figure 5, the original weld bead image is shown. At its center, the manually highlighted edges and, finally, at the right side of the image, the results of the proposed method are shown.

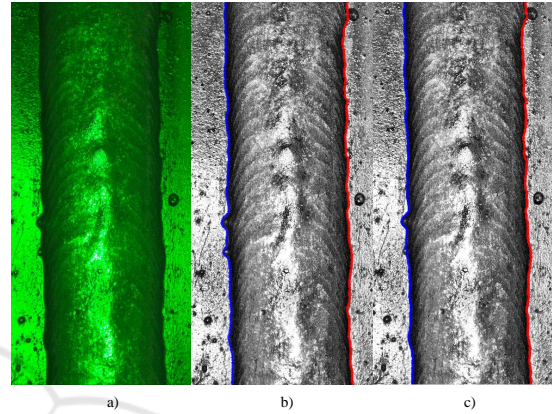


Figure 5: a) Weld bead Image. b) Manually highlighted edges. c) Proposed method highlighted edges.

Based on Figure 5 the mean error between the manually highlighted edges and the edges highlighted by the method is calculated. Thereby, the resultant absolute mean error is 2,9675 pixels for the right edge and 6,0727 pixels for the left one, as can be seen in the graphs shown in the Figures 6esquerda. Considering, based on the camera calibration, that 1 millimeter (mm) equals 46 pixels the resulting errors are 0,0645 mm and 0,1320 mm for the right and the left edges respectively. It is notable the difference between the ground truth and the proposed method result is minimal.

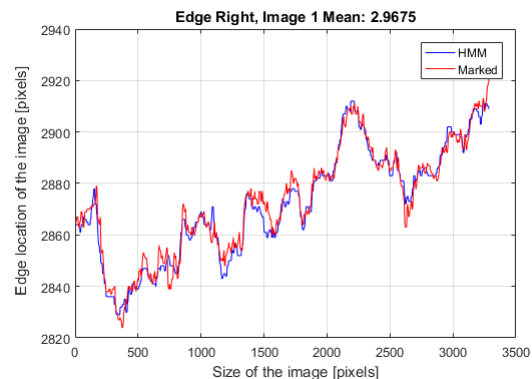


Figure 6: Graph of the difference between the manually annotated right edge and those highlighted by the method.

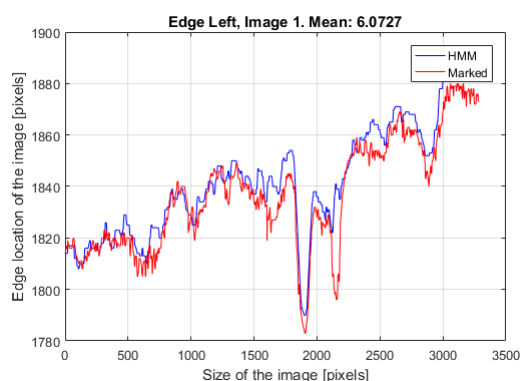


Figure 7: Graph of the difference between the manually annotated left edge and those highlighted by the method.

Lastly, the table 1 demonstrates the resultant absolute mean error in pixels (px) for the right and left sides of all tested grooves.

Table 1: Absolute average error between the manually annotated border and the border found by the method.

Welding Seams	Right Edge (px)	Left Edge (px)
1	2,9675	6,0727
2	5,1442	6,0073
3	6,4234	5,9605
4	4,4349	6,7628
5	3,5703	6,2743
6	5,8406	6,5693
7	8,9605	10,9635
8	4,5493	6,1439
9	8,2597	7,0973

5.2 Evaluation Metrics Results

In this section some evaluation metrics results are demonstrated. The results presented below were implemented using the image shown on Figure 5.

The first two metrics presented, minimum and maximum values, are able to identify points on which insufficient or excessive fusion occurs. According to American National Standards (ANS) (SOCIETY, 2001), there is a major worry about lack of fusion, since if the groove is not fully filled, the weld can be invalidated or may need another weld pass.

On Figure 8 it is possible to visualize the right weld bead edge on which there is a possible lack of fusion. It indicates the weld bead edge (highlighted in red) is too near of the empty groove line (represented by a blue line). It should be noted the parameters of minimum and maximum values may be modified by the weld inspector since the mentioned norm only

establishes the groove needs to be fully filled not specifying any minimum or maximum value.

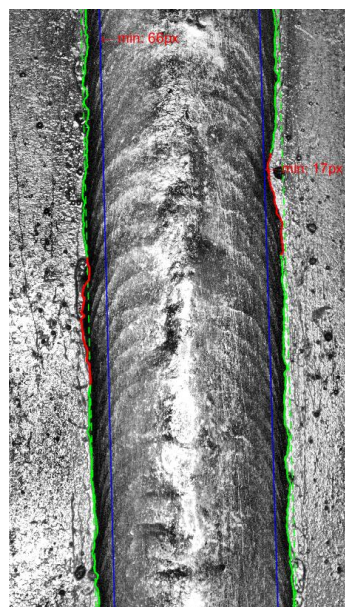


Figure 8: Results of the Minimum value metric.

Through the metric that uses the standard deviation with sliding window it is possible to graphically identify, through the peaks plotted on Figure 9, where a weld bead discontinuity may happen.

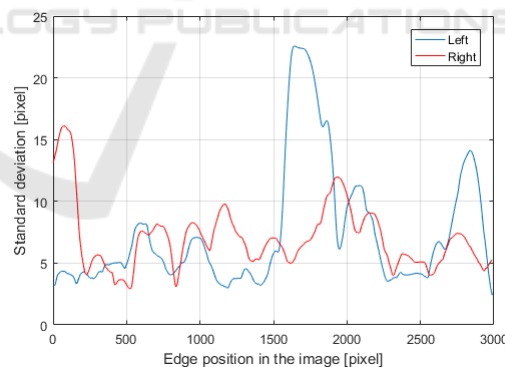


Figure 9: Graphic of the left and right weld bead edges with the standard deviation metric using sliding window.

Using the metric of the angle between the empty groove and the weld bead edge using sliding window, it is possible to identify if the weld bead exhibits an angular misalignment with respect to the empty groove. Furthermore, it is possible to visually identify the regions on which there is a greater disparity in angle. On Figure 10 it is possible to see not only these regions, but also the graph of the mentioned angle.

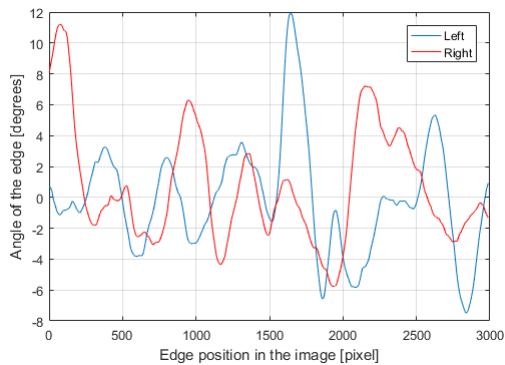


Figure 10: Graphic of the angle between the empty groove and the weld bead edge using sliding window for the left and right sides of the weld bead.

6 CONCLUSIONS

The gains provided by the welding process automation in the industry are plenty since it is a insalubrious activity for the welder who stays in contact with sparks, smoke and electricity. Therefore, it is increasingly common to use robots in this type of task since it guarantees the final process quality, increases productivity and reduces the human intervention.

Through a computer visual system attached to the linear welding robot, the presented work proposes a weld bead edge identification method and metrics to identify some discontinuities based on the weld bead geometry. The proposed method successfully identified the weld bead edges with maximum errors of 10.96 pixels. Furthermore, through the performed tests it is possible to conclude the proposed metrics contribute to identify geometric failures that may compromise the welding process.

REFERENCES

- Abendi (2014). Guia end de inspeções. <http://www.abendi.org.br/abendi/>.
- Andreucci, R. (2013). Aspectos industriais: Proteção radiológica. *Associação Brasileira de Ensaio Não Destrutivos (ABENDI)*.
- Anzai, Y. (2012). *Pattern recognition and machine learning*. Elsevier.
- Broering, C. E. et al. (2005). Desenvolvimento de sistemas para automação da soldagem e corte térmico.
- Carvalho, R. S. et al. (2009). Robô cnc para a automação da soldagem mig/mag em posições e situações de extrema dificuldade.
- Cook, G., Barnett, R., Andersen, K., Springfield, J., and Strauss, A. (1995). Automated visual inspection and interpretation system for weld quality evaluation. *Industry Applications Conference, 1995. Thirtieth IAS Annual Meeting, IAS'95., Conference Record of the 1995 IEEE*, 2:1809–1816.
- Felisberto, M. K. (2010). Técnicas automáticas para detecção de cordões de solda e defeitos de soldagem em imagens radiográficas industriais.
- Hou, X. and Liu, H. (2012). Welding image edge detection and identification research based on canny operator. In *Computer Science & Service System (CSSS), 2012 International Conference on*, pages 250–253. IEEE.
- Kumar, G. S., Natarajan, U., and Ananthan, S. (2012). Vision inspection system for the identification and classification of defects in mig welding joints. *The International Journal of Advanced Manufacturing Technology*, 61(9-12):923–933.
- Kumar, G. S., Natarajan, U., Veerarajan, T., and Ananthan, S. (2014). Quality level assessment for imperfections in gmaw. *Welding Journal*, 93(3):85–97.
- Lima, E., Castro, C. A. C., Bracarense, A. Q., and Campo, M. (2005). Determinação da relação entre parâmetros de soldagem, largura da poça e aspecto do cordão de solda utilizando câmera de alta velocidade. *soldagem Inspection-Out/Dez*, pages 182–189.
- Machado, E. (2015). Influência dos ventos sobre a qualidade das soldas realizadas em estaleiros pelo processo arame tubular.
- Schreiber, D., Cambrini, L., Biber, J., and Sardy, B. (2009). Online visual quality inspection for weld seams. *The International Journal of Advanced Manufacturing Technology*, 42(5-6):497–504.
- SOCIETY, A. W. (2001). American welding society. aws 3.0: Standard welding terms and definition.
- Steffens, C. R., Leonardo, B. Q., d. S. Filho, S. C., Hütner, V., d. Rosa, V. S., and d. C. Botelho, S. S. (2016). Welding groove mapping – implementation and evaluation of image processing algorithms on shiny surfaces. In *VISAPP 2016 11th Joint Conference on Computer Vision, Imaging and Computer Graphics Theory and Applications*, volume 3, pages 265–272.
- Sun, Y., Bai, P., Sun, H.-y., and Zhou, P. (2005). Real-time automatic detection of weld defects in steel pipe. *NDT & E International*, 38(7):522–528.